Innovative Food Science and Emerging Technologies 114 (2026) 104828

Contents lists available at ScienceDirect

Innovative Food Science and Emerging Technologies

journal homepage: www.elsevier.com/locate/ifset

Effects of emulsion pH and gas humidity on non-thermal plasma-induced lipid oxidation in oil-in-water emulsions

Danyang Liu [a], Oswaldo F. Lescano-Osorio [a], Anton Nikiforov [b], Nathalie De Geyter [b], Zdenko Machala [c], Bruno De Meulenaer [a,*]

[a] Research Group NutriFOODchem, Department of Food Technology, Safety and Health, Ghent University, Coupure Links 653, 9000 Ghent, Belgium
[b] Research Unit Plasma Technology (RUPT), Department of Applied Physics, Ghent University, Sint-Pietersnieuwstraat 41, 9000 Ghent, Belgium
[c] Division of Environmental Physics, Faculty of Mathematics, Physics and Informatics, Comenius University Bratislava, Mlynska dolina, 84248 Bratislava, Slovakia

ARTICLE INFO

Keywords:
Oil-in-water emulsions
Lipid oxidation
Non-thermal plasma
pH
Humidity

ABSTRACT

Non-thermal plasma (NTP) treatment has been researched as a food preservation technique, while lipid oxidation remains one of its concerns. In this study, oil-in-water emulsions were selected as the model system for plasma treatment to investigate the interaction between plasma induced chemistry in the aqueous phase and lipid oxidation. O/W emulsions were prepared with 10 wt% sunflower oil and 90 wt% 0.1 M phosphate solution with a pH range from 1.0 to 12.0. After dry air plasma treatment, the pH of the phosphate solution decreased mainly due to the dissolution of reactive nitrogen species in water, especially under alkaline conditions. Nitrate (NO_3^-) was the dominant species in the plasma-treated phosphate solutions. The peroxide value of extracted lipids demonstrated a bipolar distribution with peaks at pH 3.0–4.0 and 9.0, while the formation of volatile oxidation products gradually decreased as pH levels elevated. Humid air plasma enriched the amounts of H_2O_2 and NO_2^- in the liquid but lowered the level of lipid oxidation, suggesting that peroxynitrous acid chemistry contributed little to the oxidation process. Lipid oxidation in emulsions was related to the dissolution of gaseous reactive species, followed by their interactions and decomposition in the aqueous phase. The changes in pH and solute concentration affected the ionic strength, which influenced the solubility of gaseous species. O_3 is found to be the most influential species, and its concentration in the gas phase likely controls the amount of dissolved O_3 in the emulsions, thereby affecting the lipid oxidation.

1. Introduction

Thermal treatments (i.e., pasteurization and sterilization) are essential in the food industry to reduce product contamination and extend shelf-life, but they often lead to the deterioration of food's sensory and nutritional qualities, which are key concerns for today's consumers. This has shifted the research focus toward developing non-detrimental and consumer-friendly non-thermal technologies, including non-thermal plasma (NTP, also referred to as cold plasma), ultrasound, pulsed electric fields, and high-pressure processing (Jadhav et al., 2021). NTP is an ionized gas composed of free radicals, excited atoms and molecules, electromagnetic radiation (e.g., ultraviolet light), and charged particles. These reactive species can preserve foods by inactivating microorganisms through attacks on cell wall materials, cell membranes, and cellular components such as DNA and enzymes (Bayati et al., 2024; Misra & Jo, 2017).

Lipids, as one of the major macronutrients in food, are easily oxidized during food processing, leading to the deterioration of flavor and nutrition, thereby reducing food quality and causing huge economic losses (Wang et al., 2023). Therefore, lipid oxidation should be carefully monitored after NTP treatments. Previous research on NTP-treated pure oils has demonstrated the key reactive species in plasma and tracked the formation of various oxidation markers (Liu et al., 2023, 2024). However, in more complexed food systems, such as oil-in-water (O/W) emulsions, lipids are dispersed as droplets within a continuous phase of water. In such cases, gaseous plasma species first dissolve in and react with water at the gas-liquid interface, generating various species in the aqueous phase (Machala et al., 2019; Pawłat et al., 2019; Verlackt et al.,

Abbreviations: NTP, non-thermal plasma; O/W, oil-in-water; DBD, dielectric barrier discharge; RH, relative humidity; slm, standard liter per minute; POV, peroxide value; $D_{4,3}$, volume-weighted average particle diameter.

* Corresponding author.
E-mail address: Bruno.DeMeulenaer@UGent.be (B. De Meulenaer).

https://doi.org/10.1016/j.ifset.2026.104828
Received 2 May 2026; Received in revised form 29 September 2026; Accepted 29 September 2026
Available online 5 October 2026
1466-8564/© 2026 Elsevier Ltd. All rights are reserved, including those for text and data mining, AI training, and similar technologies.

2018). These dissolved and newly formed species in the aqueous phase then interact with the lipids. In addition to reactive species, the intrinsic properties of emulsion systems also influence lipid oxidation, including pH, oxygen concentration, viscosity, the presence of antioxidants, and interfacial and droplet characteristics (McClements & Decker, 2000; Villeneuve et al., 2021). For example, pH may affect lipid oxidation by altering the stability of the emulsion microstructure, the activity of lipoxygenase or antioxidants, the charge of the interfacial molecules stabilizing emulsions, and the solubility and activity of metal ions, rather than having a direct impact. In general, lipid oxidation is favored more in a low-pH environment, although contrary findings exist depending on the emulsion conditions (Bao & Pignitter, 2023; Kim et al., 2016; Li et al., 2020). The interface is important for the oxidation of emulsions, as it provides contact between lipids, oxygen, pro-oxidants, and antioxidants. Antioxidants scavenge free radicals at the interface, and negatively charged proteins (acting as emulsifiers) have been reported to show some affinity for metal ions (Hennebelle et al., 2024).

Milk is a typical example of O/W emulsions, and the effects of NTP treatment on milk have been studied by various groups. Plasma-treated milk was characterized by a fruity flavor and a fatty aroma via an electronic nose analysis. Plasma treatments applied inside the raw cow milk induced stronger microbial inactivation and lipid oxidation effects compared to treatments applied above the liquid surface (Dharini et al., 2022). The raw milk subjected to a corona discharge did not show a significant change in lipid composition. The total aldehyde content increased significantly after a 20-min treatment, but the total ketone or alcohol contents remained unchanged (Korachi et al., 2015). Compared to pasteurization (65 °C for 30 min), NTP treatment led to the absence of some carboxylic acids and the formation of aldehydes in ewe milk. Therefore, the mutton odor associated with carboxylic acids was eliminated and masked by other aromatic compounds such as aldehydes. This suggests that lipid oxidation facilitated by NTP improved the characteristic flavor of ewe milk (Wang et al., 2022). Although thermal processes impact milk quality including vitamin loss, non-enzymatic browning and protein denaturation, a non-optimized cold plasma process can also lead to quality losses in terms of lipid oxidation, protein aggregation and flavor change (Nikmaram & Keener, 2022).

Nevertheless, these studies did not elucidate the underlying oxidation mechanisms or identify the reactive species responsible for lipid oxidation in emulsions. Compared with pure lipids, emulsions are more complex systems because of the presence of the additional water matrix, which is physically positioned between the air containing the reactive plasma species and the lipids within the emulsion droplets. This implies that additional mass transfers of reactive species from the gas phase to the aqueous phase and from the aqueous phase and the emulsified lipid phase should be accounted for. In addition, intrinsic properties of emulsions, particularly pH of the water phase, may influence the effect of dissolved plasma species. Acidic conditions have been shown to enhance the antimicrobial efficacy of plasma treatment by promoting the formation of peroxynitrous acid and peroxynitric acid (Ikawa et al., 2016; Lukes et al., 2014). Furthermore, this study applies a novel plasma setup, the multi-hollow surface DBD, to generate an efficient and non-detrimental discharge using an industrially relevant, readily available, and cheap gas (air). This configuration enables the use of humidified air, thereby increasing the diversity of reactive species and facilitating the identification of important species. Increasing gas humidity significantly decreases ozone but increases HNO_3 concentrations in the gas phase (Cimerman & Hensel, 2023; Liu et al., 2024). This change is expected to alter the reactive species composition in the aqueous phase and affect lipid oxidation in emulsions. To investigate these factors, emulsions with different pH values were treated using dry and humid air plasma in this study. Beyond the pH range typically encountered in food systems (approximately pH 3.0–8.0), extreme pH conditions on both acidic and alkaline sides (pH 1.0–12.0) were investigated to gain mechanistic insights into the interactions among plasma chemistry, emulsion properties, and lipid oxidation process. Lipid oxidation products and reactive species in the aqueous phase were quantified subsequently. A simplified oil-in-water emulsion system was selected as the model system to eliminate the influence of other components present in real food systems, such as proteins and carbohydrates, which can participate in oxidation reactions and interact with lipids (McClements & Decker, 2000).

2. Materials and methods

2.1. Chemicals and materials

The impact of plasma treatment on different oils had been illustrated in a previous study (Liu et al., 2024). Sunflower oil was selected in this study as a moderately unsaturated oil. Organic sunflower oil was purchased from the local market (Delhaize, Belgium), with the following fatty acid composition: C18:2 (53.7%), C18:1 (35.6%), C16:0 (6.0%), C18:0 (3.5%), C22:0 (0.6%), and C20:0 (0.5%). Hexanal, nonanal, Tween 20, titanium(IV) oxysulfate, Griess reagents, indigo potassium trisulfonate, and 2,6-dimethylphenol were obtained from Sigma-Aldrich (Belgium & Slovakia). Hexanal-d_{12} and nonanal-d_{18} were obtained from CDN isotopes (Canada). Iso-propanol, isooctane, sodium sulphate, $Na_2HPO_4{\cdot}7H_2O$, and $NaH_2PO_4{\cdot}H_2O$ were purchased from Chem Lab (Belgium). All chemicals and reagents were of analytical purity or better.

2.2. Sample preparations

Initially, a 0.1 M sodium phosphate solution (pH 7.0) was prepared and then adjusted to pH values of 1.0, 2.0, 3.0, 4.0, 5.0, 6.0, 7.0, 8.0, 9.0, 10.5, and 12.0 using aqueous HCl or NaOH solutions. The surfactant (1 wt% Tween 20) was then dispersed in the phosphate solutions. A mixture consisting of 10 wt% sunflower oil and 90 wt% surfactant-phosphate solution was pre-emulsified by blending with an Ultra-Turrax (Janke and Kunkel, IKA-Werk, Germany) at 10,000 rpm for 10 min. Finally, the mixture was homogenized seven times using a high-pressure valve, two-stage homogenizer (APV-1000, APV Benelux NV/SA, Belgium) at 250 bar/30 bar. The ratio of surfactant, oil, and buffer solution, together with the preparation method, followed a previously described method to ensure emulsion stability (Vandemoortele & De Meulenaer, 2015).

2.3. NTP treatment

The NTP apparatus was the same surface dielectric barrier discharge (DBD) reactor as described by Liu et al. (2023). Approximately 2.0 g of emulsion sample (around 1.6 mm thick) was weighed in a glass petri dish (Ø 50 mm) and treated by the plasma discharge. A 2 g sample was chosen in this study to maximize the treatment efficiency while ensuring complete coverage of the petri dish. Several operational plasma parameters were kept constant during this study including treatment time (120 s), power (around 14 W), and plasma-sample distance (15 mm). To treat emulsion samples with different pH levels, plasma was generated in dry air (synthetic air, Air Products) at a flow rate of 5 standard liters per minute (slm). The pH change of phosphate solutions treated with dry air plasma was measured with a pH meter (Schott Instruments, Germany). Plasma was also generated in air with varying humidity (0, 35, and 93% RH) at a flow rate of 2 slm, and then applied to the emulsion sample at pH 7.0. The process parameters were selected based on a previous study (Liu et al., 2024) and resulted in a suitable amount of oxidation products for analysis. The same plasma treatments used for the emulsion samples were applied to phosphate solutions to determine the plasma species, except that the 93% RH air was replaced with 99% RH air in the humid air plasma condition. The adjustments to flow rate and RH were made because the determination of plasma species was conducted in a different lab, where the experimental methods for controlling these parameters differed.

2.4. Analytical methods

2.4.1. Peroxide value (POV)

The radicals in the plasma discharge (e.g., $^{\bullet}NO_2$, and $^{\bullet}NO_3$) or solution (e.g., $^{\bullet}OH$) can initiate lipid autoxidation and generate lipid hydroperoxide, a primary oxidation product measured by POV (Frankel, 2005; Liu et al., 2023). Each NTP-treated emulsion was first transferred to a test tube containing a thin layer of NaCl. 5 mL of isooctane/isopropanol (3,1, *v*/v) was used to rinse the petri dish containing NTP-treated emulsion and then transferred to the same test tube. The mixture was vortexed for 30 s, and the isooctane phase was transferred to a previously dried and weighed flask with a ground joint. The extraction was repeated two more times following the same procedure. Similarly, 2.0 g of non-treated sample was weighed in a test tube containing NaCl and directly extracted three times. The extract was rotaevaporated at 20 °C under vacuum, and kept under nitrogen for 30 min. The weight of the lipid extract in the flask was calculated by comparing the weight difference of the flask. The POV of the extracted lipids was determined by titration based on an official method of the American Oil Chemists' Society (Method Cd 8b-90).

2.4.2. Hexanal and nonanal quantification

Ozonolysis of C=C double bonds in fatty acid chains leads to the formation of carbonyls, with hexanal and nonanal being the characteristic products (Liu et al., 2023). The hexanal and nonanal contents were quantified using headspace solid-phase microextraction combined with gas chromatography–mass spectrometry. An aliquot of 50.0 or 100.0 μL of the NTP-treated emulsion, depending on the extent of oxidation, was used for quantification following the previously described procedures (Liu et al., 2023). Hexanal-d_{12} and nonanal-d_{18} were incorporated into the sample as internal standards. The oven program of the gas chromatograph was slightly modified as follows: initially set at 50 °C for 5 min, and then increased to 140 °C at a rate of 4.5 °C/min. External calibration curves ($n \geq 3$) of hexanal and nonanal were prepared using non-NTP treated samples as a matrix. The standard deviation (SD) of residuals and the slope of the calibration curve were calculated, and the limit of detection (LOD) was then determined as 3.3 x (SD/slope). The average LODs for hexanal and nonanal were 1.9 and 5.6 μg/g emulsion, respectively, which were lower than the amounts detected in all NTP-treated emulsions. The concentrations of these volatile oxidation products were below the LOD in the non-treated emulsions at each pH.

2.4.3. Aqueous species determination

The concentrations of H_2O_2, O_3, $NO_2^-$and NO_3^- in the treated phosphate solutions were measured using a Shimadzu UV-1900 UV–Vis spectrophotometer according to the procedures described before (Pareek et al., 2024; Tarabová et al., 2018). Briefly, H_2O_2 reacted with titanium(IV) oxysulfate under acidic condition to form a yellow-colored product with maximum absorption at 407 nm, O_3 decolorized the indigo potassium trisulfonate dye which has maximum absorbance at 600 nm, and NO_2^- reacted with Griess reagents under acidic condition to form a deep purple azo compound with maximum absorption at

540 nm. In addition, the concentration of NO_3^- was measured through the reaction with 2,6-dimethylphenol under strong acidic conditions. The nitration product of 2,6-dimethylphenol, 4-nitro-2,6-dimethylphenol, was quantified using its maximum absorption at 337 nm. Since NO_2^- was also converted to NO_3^- in this strong acid condition, the actual concentration of NO_3^- was calculated by subtracting the measured concentration of NO_2^- from the concentration of NO_3^-. External calibration curves of NO_2^-, H_2O_2, and NO_3^- were determined, followed by the calculation of the SD of residuals and the slope of the calibration curve. The LODs were then calculated as 3.3 x (SD/slope) for NO_2^- (0.8 μmol/L), H_2O_2 (29.6 μmol/L), and NO_3^- (100 μmol/L). The calibration ranges were 0.8–50 μmol/L for NO_2^-, 29.6–1000 μmol/L for H_2O_2, and 100–1000 μmol/L for NO_3^-. The concentration of plasma-treated phosphate solution used for measurements was adjusted to fit in the calibration range. The quantifiable O_3 concentration ranged from 0.2 to 2.1 μmol/L, as reported by Baird et al. (2017).

2.4.4. Particle size measurement

The particle sizes of emulsions before and after NTP treatment were analysed using a Mastersizer 3000 (Malvern Instruments Ltd., UK), with a refractive index of 1.47 and an absorption index of 0.01 assumed for sunflower oil.

2.5. Statistical analyses

All NTP treatments and subsequent analyses were performed in at least three replicates, and results are represented as the means of replicates. The Shapiro-Wilk test and the Levene's test were used to assess the data for normal distribution and homoscedasticity, respectively. One-way analysis of variance was then performed to identify differences among the samples. When differences were detected, multiple comparisons were conducted using the Tukey-b test in case of homoscedasticity or the Games-Howell test in case of heteroscedasticity. Moreover, *t*-tests were applied to check whether NTP treatment introduced significant changes in the pH of the phosphate solution and the POV of emulsions at each pH level. A *p*-value less than 0.05 was applied to calculate the statistical significance for all comparisons. The statistical analyses were processed by the SPSS 28 statistics package (IBM, SPSS, Inc.).

3. Results and discussions

3.1. Impact of initial phosphate solution pH

3.1.1. pH change of phosphate solutions

The pH change of phosphate solutions subjected to dry air plasma is illustrated in Fig. 1. According to the one sample *t*-test, phosphate solutions with an initial pH level between 3.0 and 12.0 exhibited a statistically significant pH drop due to plasma treatment, in contrast to solutions at pH 1.0 and 2.0. The pH drop can be attributed to the dissolution of gaseous NO, NO_2, and N_2O_5 formed in the plasma, which then react with water to release protons (eqs. (1), (2), and (3)) (Machala et al., 2019). Higher buffering capacity is expected when the pH of a phosphate solution is closer to the pKa values of H_3PO_4, $H_2PO_4^-$, and HPO_4^{2-}, which are around 2.1, 7.0, and 12.5, respectively (Z. C. Liu et al., 2019). A more noticeable pH drop of 0.66 was observed at pH 10.5, as it was distant from both pKa_2 (7.0) and pKa_3 (12.5) (Fig. 1). Compared to

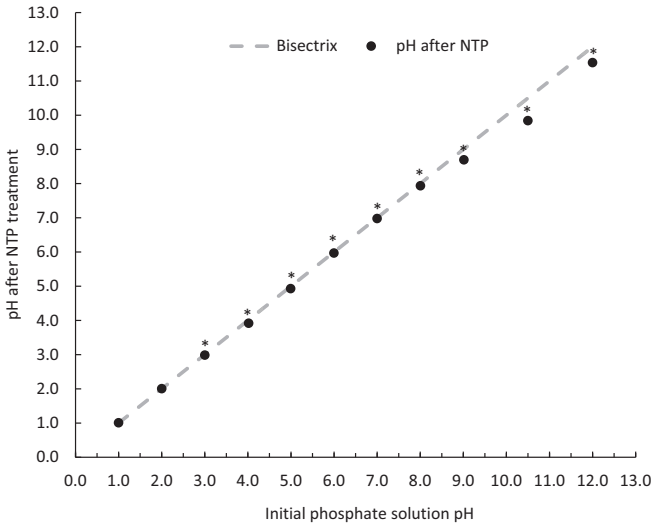

Fig. 1. Change in the pH of phosphate solutions due to dry air NTP treatment ($n = 3$). Asterisk (*) indicates a significant difference in the solution pH after NTP treatment ($p < 0.05$).

acid solutions, larger drops in pH were observed under alkaline conditions, probably because the low amount of H^+ in alkaline solutions could facilitate eqs. (1), (2), and (3). Therefore, the pH change in alkaline (liquid) food should receive more attention after plasma treatment. Significant decreases in pH were also previously demonstrated in juice (from 4.0 to 3.0) and milk (from 6.7 to 6.2) treated by DBD plasma (Wu et al., 2021; Xiang et al., 2018).

$$2NO_2(aq) + H_2O \rightarrow NO_2^- + NO_3^- + 2H^+ \quad (1)$$

$$NO(aq) + NO_2(aq) + H_2O \rightarrow 2NO_2^- + 2H^+ \quad (2)$$

$$N_2O_5(aq) + H_2O \rightarrow 2NO_3^- + 2H^+ \quad (3)$$

3.1.2. Oxidative status under different pHs

The POV of the extracted fat from emulsions treated with dry air plasma and the control samples under different pH values is illustrated in Fig. 2. Independent samples *t*-tests confirmed that the NTP-treated emulsions exhibited significantly higher POV than the control sample at each pH level, indicating that NTP treatment promoted lipid oxidation in emulsions. The POV of NTP-treated emulsions followed a bipolar distribution as pH increased, with the first peak at pH 3.0 and 4.0, and a second, lower peak at pH 9.0. The POV of the control samples exhibited significant but limited differences. To explain the changes in POV, ionic strength in phosphate solution was calculated and will be further discussed in Section 3.3.1.

Liu et al. (2024) have reported that ozonolysis of C=C double bonds in fatty acid chains leads to the formation of carbonyls, and hexanal and nonanal which are the characteristic products of the ozonolysis of C18:2 and C18:1, respectively. The unsaturated fatty acids present in the sunflower oil used for emulsion preparation mainly consist of C18:2 (53.7%) and C18:1 (35.6%). Therefore, the concentrations of hexanal and nonanal in the plasma-treated emulsions were measured after subjecting emulsions at pH 1.0, 3.0, 7.0, 9.0, and 12.0 to dry air plasma (Fig. 3). The amount of the two volatile oxidation products followed the same trend: more were generated in the acid environment at pH 1.0 and 3.0 and less were formed as pH increased further. This trend will be explained later in Section 3.3. In all cases, the hexanal concentration was lower than the nonanal concentration on a weight basis (Fig. 3) and on a molar basis (data not shown), despite the higher amount of C18:2 fatty acid present in the sunflower oil. Since C18:2 fatty acid contains one more C=C double bond than C18:1 fatty acid, the ozonolysis on the C18:2 fatty acid chain can occur at both ω-9 and ω-6 positions, leading to a more diverse carbonyl composition and a reduced formation of individual carbonyl compounds (e.g., hexanal) (Liu et al., 2024).

3.1.3. Particle sizes

Droplet size determines the oil–water interfacial area available for oxygen diffusion and contact with pro-oxidants. For a fixed oil-to-water ratio in an emulsion system, smaller droplets provide a larger interfacial area, thereby promoting lipid oxidation, although some studies have reported contradictory findings (ten Klooster et al., 2024). This study examines whether pH conditions or plasma treatment impact particle size in emulsion. The particle size distribution of emulsions at pH 1.0, 3.0, 7.0, 9.0, and 12.0 were measured before conducting plasma treatment (Table S1). Volume-weighted average particle diameter ($D_{4,3}$), ranging from 0.5 to 0.6 μm, exhibited no significant difference among the control samples, indicating that pH levels did not affect the particle size of emulsions, and that sample preparation was performed consistently. Furthermore, plasma treatment did not significantly affect particle size (Table S1). Since particle size is recognized as a key factor for emulsion stability, these results suggest that stability was not affected by either pH adjustment or NTP treatment. Therefore, the differences in oxidation status among emulsions at various pH levels should be related to other factors, such as the plasma chemistry in the emulsions.

3.1.4. Effect of pH on aqueous species

Plasma species in the gas phase can interact with the liquid, triggering chemical reactions that generate additional secondary active species (Dharini et al., 2023). These species in the aqueous phase (i.e., phosphate solution in this study) could influence lipid oxidation in

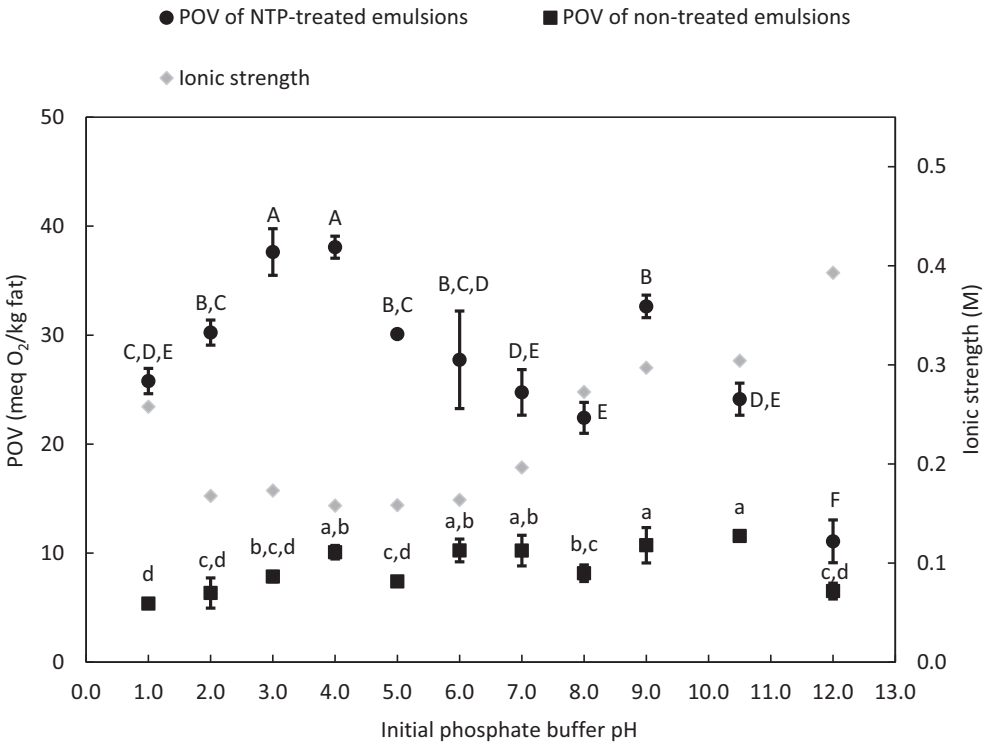

Fig. 2. Impact of initial phosphate solution pH on the POV of emulsions before and after dry air NTP treatment ($n = 3$) and on ionic strength in phosphate solution. Capital and lowercase letters indicate significant differences ($p < 0.05$) in the POV for NTP-treated and non-treated samples, respectively.

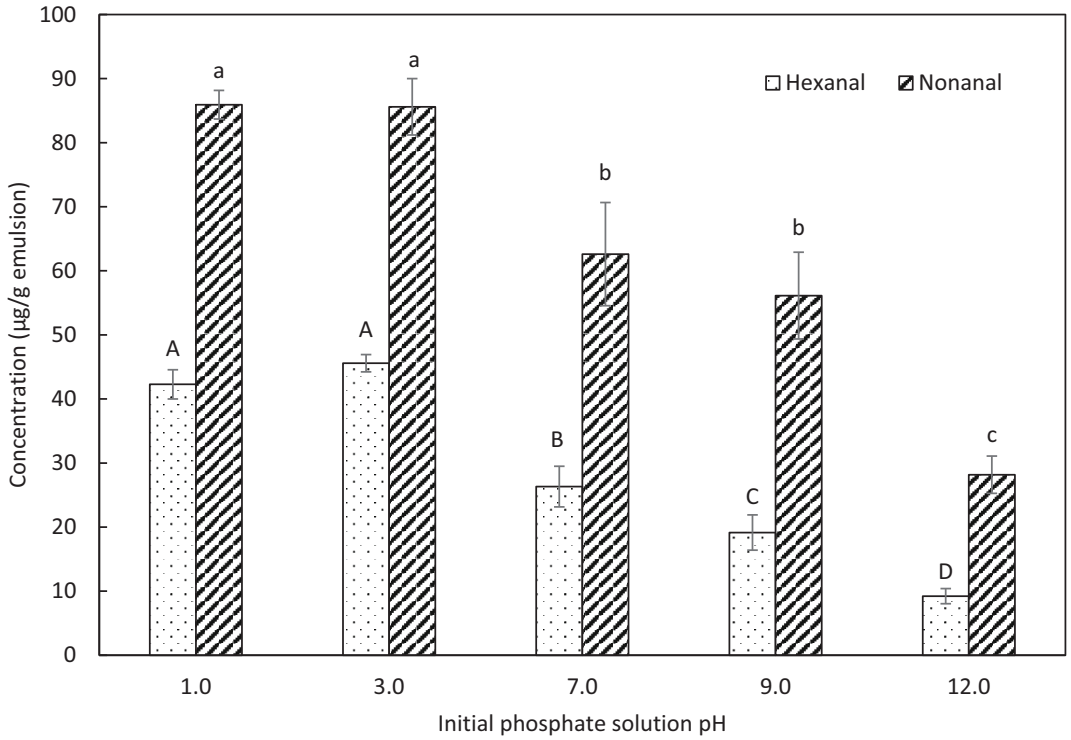

Fig. 3. Impact of initial phosphate solution pH on the volatile oxidation products in emulsions treated with dry air plasma ($n = 3$). Capital and lowercase letters indicate significant differences ($p < 0.05$) in the concentrations of hexanal and nonanal, respectively.

emulsions, as the initiation of oxidation occurs at the oil-water interface. To elucidate the oxidative status in relation to aqueous plasma chemistry, the concentrations of H_2O_2, O_3, NO_2^-, and NO_3^- in the NTP-treated phosphate solutions at pH 1.0, 3.0, 7.0, 9.0, and 12.0 were measured (Table 1). The main formation pathways of NO_2^- and NO_3^- are the dissolution of gaseous NO, NO_2, and N_2O_5 formed in the plasma discharge (eqs. (1), (2), and (3)) (Machala et al., 2019). The most abundant species was NO_3^-, which was two orders of magnitude higher than the NO_2^- content. This suggests that eq. (3) may occur more frequently than eqs. (1) and (2). This can be due to the higher Henry's solubility constant and concentration of N_2O_5(g) compared to NO(g) and NO_2(g) (Liu et al., 2023; Sander, 2023). As no HNO_3(g) was detected in the dry air plasma (Liu et al., 2023), it confirms that NO_3^- in phosphate solution treated with dry air plasma was formed by the reaction of gaseous nitrogen species (e.g., $^{\bullet}NO_2$ and N_2O_5) with water, rather than being formed in the gas phase and then dissolving into the liquid phase.

Although O_3 is the dominant species in the gas phase (Cimerman & Hensel, 2023; Liu et al., 2023), it was only detected in limited amounts in the acidic solutions (Table 1). This could be explained by the low solubility of O_3: the Henry's constant of O_3 is about seven orders of magnitude lower than that of gaseous H_2O_2 and HNO_3 (Sander, 2023). The low concentration of NO_2^- suggests the dissolution of O_3, as dissolved O_3 can readily oxidize NO_2^- to NO_3^- in solution (eq. (4)) (Zhou et al., 2020).

$$O_{3\,(aq)} + NO_2^- \rightarrow NO_3^- + O_{2\,(aq)} \quad (4)$$

The amount of H_2O_2 was restricted in the NTP-treated solutions at all pH levels (Table 1). H_2O_2 is dominantly produced by the recombination of $^{\bullet}OH$ radicals formed through water dissociation (cf. Section 3.2.2). However, for dry air plasma treatment, the input gas contained no water, and the powerful short-living plasma species did not reach the liquid phase (Liu et al., 2023), thus water dissociation was very limited. By contrast, the measurable H_2O_2 quantity in case of highest RH confirms the importance of gas-phase H_2O in H_2O_2 production.

3.2. Impact of air relative humidity

3.2.1. Oxidative status in relation to relative humidity

Plasma was generated using air at different RH with a constant flow rate of 2 slm and applied to emulsions at pH 7.0. The POV of emulsions demonstrated a declining trend with increasing air RH (Table 2).

Table 1
Impact of pH and air RH on the aqueous species concentrations in phosphate solution after plasma treatment ($n \geq 3$). Results are expressed as mean values ± SD. Superscript letters indicate significant differences ($p < 0.05$) within each column, shown separately for the groups of solution pH and air RH.

Plasma parameters	Phosphate solution pH	Concentration of aqueous species (μmol/L)			
		H_2O_2	O_3	NO_2^-	NO_3^-
Dry air, flow rate of 5 slm	1.0	< LOD*	0.6 ± 0.3 ^{a}	1.7 ± 0.1 ^{a}	300.5 ± 9.5 ^{a}
	3.0	< LOD	0.3 ± 0.2 ^{a}	1.3 ± 0.3 ^{a}	301.4 ± 11.7 ^{a}
	7.0	< LOD	< 0.2	1.0 ± 0.3 ^{a}	322.4 ± 13.5 ^{a}
	9.0	< LOD	< 0.2	1.3 ± 0.5 ^{a}	340.0 ± 7.6 ^{a}
	12.0	< LOD	< 0.2	1.7 ± 0.5 ^{a}	321.4 ± 35.1 ^{a}
Dry air at 2 slm		< LOD	< 0.2	1.8 ± 0.4 ^{A}	1567.2 ± 142.7 ^{A}
35% RH air at 2 slm	7.0	< LOD	< 0.2	278.6 ± 17.9 ^{B}	1587.9 ± 187.2 ^{A}
99% RH air at 2 slm		36.3 ± 3.5	< 0.2	406.2 ± 63.6 ^{B}	1283.4 ± 171.0 ^{A}

* 29.6 μmol/L.

Table 2
The POV of emulsions at pH 7.0 treated with air plasma in different RH and the control ($n = 3$), expressed as mean values ± SD. Superscript letters indicate significant POV differences ($p < 0.05$).

Plasma parameters	POV (meq O_2/kg fat)
Dry air at 2 slm	26.8 ± 0.9 [a]
35% RH air at 2 slm	18.3 ± 2.3 [b]
93% RH air at 2 slm	13.1 ± 0.5 [c]
Control	8.0 ± 0.5 [d]

Similarly, the concentrations of hexanal and nonanal exhibited the same trend with respect to air RH (Fig. 4). These results will be further discussed in Section 3.3. The POV of NTP-treated samples was significantly higher than that of the control, indicating that lipid peroxidation was initiated by all plasma treatments regardless of air RH. Comparably, the bactericidal effect was also less pronounced when the air plasma humidity was increased from 0% to 75% (De Baerdemaeker et al., 2023).

3.2.2. *Effect of air relative humidity on aqueous species*

In humid air plasma, water vapors can dissociate to form $^{\bullet}OH$ radicals through processes such as electron-impact dissociation (Eq. (5)) and reaction with $O^{\bullet}$ (Eq. (6)) (Bruggeman & Schram, 2010). $^{\bullet}OH$ radicals can recombine to form H_2O_2 (eq. (7)), which dissolves in the liquid phase and was detected under highest RH (99% RH) (Table 1). $^{\bullet}OH$ radicals also react rapidly with $^{\bullet}NO$ and $^{\bullet}NO_2$ to form HNO_2 and HNO_3 (eqs. (8) and (9)) in the gaseous phase, which then quickly dissolve in water and contribute to the formation of NO_2^- and NO_3^- (Wandell et al., 2019). Compared to dry air plasma, more HNO_2 is typically observed in the gaseous phase of humid air plasma (Janda et al., 2021). This explains the increase in NO_2^- with rising RH observed here (Table 1). Additionally, as RH increased, the amount of O_3 in humid air plasma decreased (Cimerman & Hensel, 2023; Liu et al., 2023), which likely restricted the oxidation of NO_2^- to NO_3^- (eq. (4)), leading to a higher concentration of NO_2^- and slightly lower concentration of NO_3^- in the solutions.

Besides eq. (4), NO_3^-(aq) can also originate from the direct dissolution of gaseous HNO_3, whose concentration increases with elevated RH (Cimerman & Hensel, 2023; Schmidt-bleker et al., 2016). Gaseous HNO_3 can be produced via eq. (9) and also from N_2O_5(g) through eq. (10). Notably, the reaction between N_2O_5 and H_2O can occur in the gas phase (eq. (10)) and the liquid phase (eq. (3); N_2O_5 is highly soluble in water), both contributing to the formation of NO_3^- in the solution. The final concentration of NO_3^-(aq) was not significantly affected by the RH of input gas (Table 1), indicating that the formation pathways of NO_3^-(aq) are counterbalanced under different RH conditions. Additionally, the NO_3^- concentration was remarkably higher when treating solution with dry air plasma at a lower flow rate (i.e., 2 slm compared to 5 slm). Lowering the flow rate can cause an increase in the specific energy input, shifting the plasma chemistry from an ozone mode to an NO_x mode, a phenomenon known as the discharge poisoning effect (Fridman, 2008), explaining the higher NO_3^- concentrations at 2 slm in dry air. The WHO guidelines for nitrate and nitrite in drinking-water are 50 mg/L (806 μmol/L) and 3 mg/L (65 μmol/L), respectively (WHO, 2016). Therefore, the nitrate and nitrite concentrations in the phosphate buffer treated with dry air plasma (5 slm) remained within the acceptable limits, whereas a lower flow rate caused the NO_3^- concentration exceeding the limit, and humid air plasma treatment further led to the NO_2^- concentration exceeding the limit. Toxicological concerns should be raised following these exceedances. For example, nitrite can act as a nitrosylating agent and react with secondary or tertiary amines to form N-nitrosamines, which exhibit toxic, carcinogenic, and mutagenic properties (Manchuri et al., 2024). Nitrosotyrosine was detected after

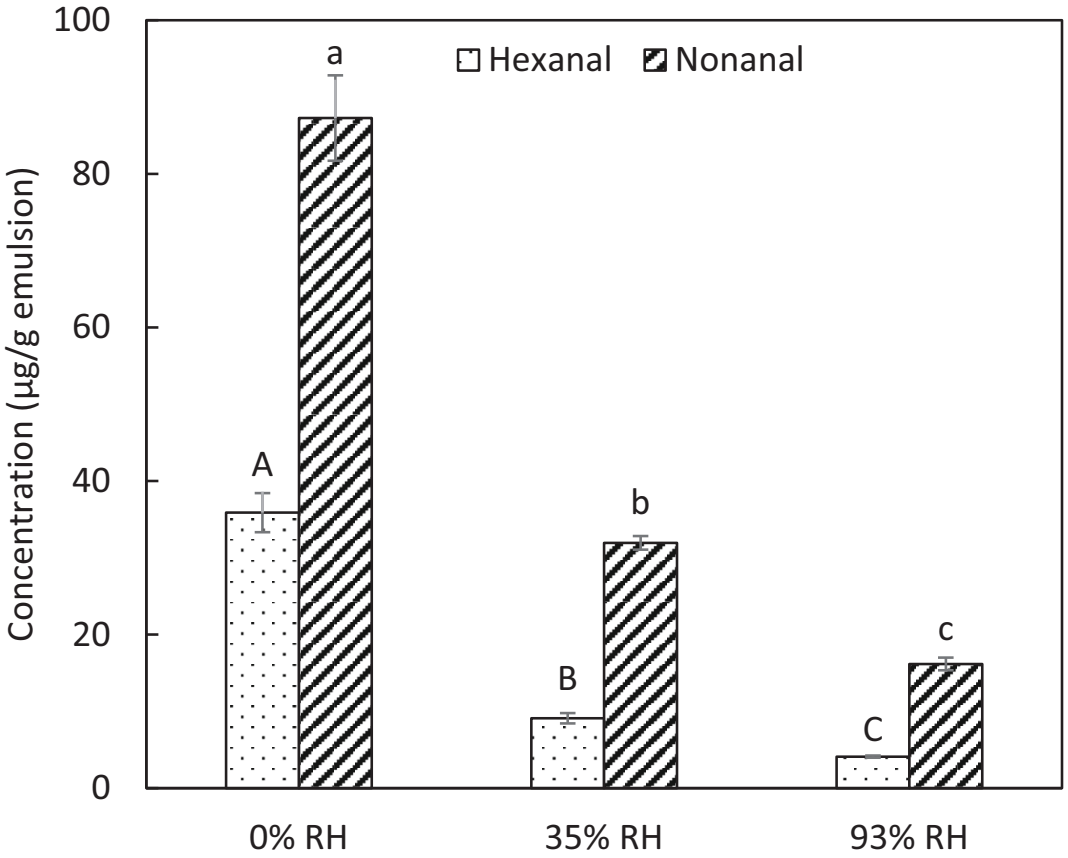

Fig. 4. Volatile oxidation products in emulsions at pH 7.0 treated with air plasma in different RH ($n = 3$). Capital and lowercase letters indicate significant differences ($p < 0.05$) in the hexanal and nonanal concentrations, respectively.

the application of a similar plasma treatment to a tyrosine solution, indicating that nitration reactions occur at the amino-acid level (Sierens et al., 2026).

$$e^- + H_2O \rightarrow OH + H + e^- \quad (5)$$

$$O + H_2O \rightarrow OH + OH \quad (6)$$

$$OH + OH \rightarrow H_2O_2 \quad (7)$$

$$OH + NO \rightarrow HNO_2 \quad (8)$$

$$OH + NO_2 \rightarrow HNO_3 \quad (9)$$

$$N_2O_5(g) + H_2O \rightarrow 2HNO_3(g) \quad (10)$$

3.3. Correlation between aqueous species and lipid oxidation

3.3.1. Solubility of gaseous species

When emulsions and phosphate solutions at various pH levels were subjected to dry air plasma, the concentration of measured aqueous species did not change with pH levels in the solution (Table 1), nor did it correlate with the oxidation level in emulsions at different pH values (Fig. 2 and Fig. 3). In dry air plasma, O_3, $^{\bullet}NO_2$, $^{\bullet}NO_3$, and $^1O_2$ were identified as the main reactive species, and O_3 was the most abundant gaseous species (Liu et al., 2023). Despite the low concentration detected in the solution, O_3 is presumed to have dissolved and reacted with components in the solution (cf. Section). The solubility of O_3 in water is highest between pH 2.0 and 6.0, gradually decreasing at pH levels below 2.0 and above 6.0 under different decomposition mechanisms in acidic and alkaline solutions (Egorova et al., 2015). The reported O_3 solubility aligned with the amounts of volatile oxidation markers across pH levels in NTP-treated emulsions (Fig. 3). This indicates that ozonolysis occurred in the emulsions due to the dissolved O_3, and that the extent of this reaction was influenced by the emulsion pH. $^{\bullet}OH$ radicals are produced via ozone decomposition in water through a series of chain reactions, and the time-integrated concentration of $^{\bullet}OH$ (mol dm^{-3} s) is known to decrease from pH 3.0 to 9.0 and slightly increase at pH 10 (Khuntia et al., 2015). This trend was similar with the POV in NTP-treated emulsions (Fig. 2), suggesting that the radicals generated by O_3-water interactions contributed to the formation of lipid hydroperoxides. Similar to O_3, the solubility of other gaseous species in the emulsions can potentially affect the degree of lipid oxidation within the emulsions. For example, the conversion of dissolved $^{\bullet}NO_2$ to NO_2^- and NO_3^- is less favorable in acidic environments, as the high concentration of H^+ shifts eqs. (1) and (2) backward, thereby preserving dissolved $^{\bullet}NO_2$ and promoting greater oxidation compared to alkaline conditions.

As ionic strength is inversely related to O_2 solubility (Xing et al., 2014), the aqueous pH may influence lipid oxidation by affecting the solubility of gaseous plasma species through ionic strength. The total ionic strength in phosphate solution at each pH was thus calculated considering the Na^+, H^+, Cl^- (introduced through HCl and NaOH for pH adjustment), and phosphate anions present in the solution, using eq. (11),

$$I = \frac{1}{2}\sum_{i=1}^{n} C_i Z_i^2 \quad (11)$$

where C_i is the molar concentration of ion i and Z_i is the charge number of ion i. The ionic strength as a function of pH shows an almost opposite trend to the POV of NTP-treated emulsions as a function of pH (Fig. 2), with the Pearson correlation coefficient (r) as −0.745. This indicates a strong negative correlation between pH-dependent ionic strength and POV ($p < 0.01$). The solubility of gases in aqueous salt solutions generally diminishes with increasing salt concentration, known as the salting-out effect. To further investigate the impact of salt concentration and ionic strength on lipid oxidation, emulsions were prepared with 0.01 M, 0.1 M, 0.3 M, and 0.5 M phosphate solution at pH 3.0 and treated with the same NTP. The POV and the concentrations of volatile oxidation products after NTP treatments are presented in Table 3. The POV shows a decreasing trend with higher phosphate concentrations and ionic strengths, suggesting that the solubility of gaseous reactive species affected by ionic strength influences the extent of oxidation in emulsions. Compared to POV, the concentrations of hexanal and nonanal are less sensitive to changes in ionic strength. This difference could be attributed to the fact that the formation of volatile oxidation products is primarily related to dissolved ozone, whereas the solubility of other gaseous species besides ozone also affects POV.

3.3.2. Effect of humidity

The level of lipid oxidation in emulsions at pH 7.0 diminished with increasing air plasma humidity (Table 2 and Fig. 4), but it contrasts with the change in the concentrations of H_2O_2 and NO_2^- in the plasma-treated solution (Table 1). However, the trend of lipid oxidation aligns with the O_3 concentration in the gas phase. The rise in RH reduced the gaseous O_3 concentration (Cimerman & Hensel, 2023; Liu et al., 2023), which likely resulted in a lower amount of dissolved O_3 in the liquid phase. This, in turn, explains the reduced level of lipid oxidation and reinforces the role of O_3 as a key reactive species driving lipid oxidation in emulsions. Therefore, the humidity of air plasma indirectly affected the aqueous-phase species and lipid oxidation by influencing the gaseous species composition.

Interestingly, the POV of pure oils increased with elevated RH (Liu et al., 2023), thus emulsions and pure oils reacted differently to humid air plasma. For humid air plasma treatment, the formation of lipid hydroperoxide (contributor to the POV value) in pure oils was mainly related to peroxynitrous (ONOOH) and/or peroxynitric (O_2NOOH) acids (Liu et al., 2023). These acids can decompose into radicals (eqs. (12) and (13)) (Ikawa et al., 2016; Lukes et al., 2014), which can directly initiate lipid oxidation in pure oils by abstracting hydrogen atoms from allylic carbons. However, in O/W emulsion systems, the impact of these radicals (e.g., $^{\bullet}OH$ and $^{\bullet}NO_2$) was probably mitigated first in the water phase via processes such as eq. (7). Alternatively, peroxynitrous acid may rapidly isomerize to nitric acid in emulsions, which does not decompose into radicals (Goldstein et al., 2005).

3.3.3. Peroxynitrous acid chemistry

H_2O_2 and NO_2^- in plasma-treated water have been reported to exhibit antibacterial effects, which are enhanced at acidic pH through the facilitated formation of peroxynitrous acid via eq. (14) (Lukes et al., 2014; Machala et al., 2013). Nevertheless, in our study, the rising amounts of H_2O_2 and NO_2^- in the phosphate solution treated with humid air plasma were accompanied by a reduced level of lipid oxidation in the emulsion. To determine whether an acidic pH would facilitate the formation of peroxynitrous acid and subsequently impact lipid oxidation, the same plasma treatment with 93% RH air was applied to emulsions at pH 3.0 and 7.0. The POV (meq O_2/kg fat) for two emulsions, 13.9 ± 0.6 at pH 3.0 and 13.1 ± 0.5 at pH 7.0, did not show a significant difference.

Table 3
Impact of phosphate concentration and ionic strength in the solution (pH 3.0) on the POV and volatile oxidation markers for emulsions. Results are expressed as mean values ± SD ($n = 3$). Superscript letters indicate significant differences ($p < 0.05$) within each column.

Phosphate concentration (M)	Ionic strength (M)	POV (meq O_2/kg fat)	Hexanal concentration (μg/g emulsion)	Nonanal concentration (μg/g emulsion)
0.01	0.02	35.6 ± 0.9 ^{a}	77.5 ± 7.4 ^{a}	84.3 ± 2.1 ^{a}
0.1	0.16	31.7 ± 0.7 ^{b}	69.5 ± 3.3 $^{a, b}$	87.3 ± 4.7 ^{a}
0.3	0.47	26.5 ± 1.2 ^{c}	59.8 ± 5.4 $^{b, c}$	67.5 ± 2.3 ^{b}
0.5	0.79	18.4 ± 1.0 ^{d}	51.0 ± 2.7 ^{c}	65.5 ± 4.6 ^{b}

Further NTP treatment at a closer distance (6 mm instead of 15 mm) generated approximately double the amounts of H_2O_2 and NO_2^-, but the POV (meq O_2/kg fat) of emulsions at pH 3.0 (14.8 ± 0.6) and 7.0 (16.0 ± 0.9) did not exert a significant difference either. These results may be attributed to the low amount of peroxynitrous acid formed or its rapid isomerization to nitric acid in emulsions. Overall, the peroxynitrous acid chemistry (involving H_2O_2 and NO_2^-) had a restricted impact on lipid oxidation in emulsions compared to O_3.

$$O = NOOH \rightleftharpoons {}^{\bullet}OH + {}^{\bullet}NO_2 \quad (12)$$

$$O_2NOOH \rightleftharpoons HO_2^{\bullet} + {}^{\bullet}NO_2 \quad (13)$$

$$NO_2^- + H_2O_2 + H^+ \rightarrow O = NOOH + H_2O \quad (14)$$

4. Conclusion

Oil-in-water (O/W) emulsions were prepared at different pH levels and subjected to NTP generated in both dry and humid air. Gaseous plasma species interacted with the liquid phase, generating various aqueous-phase species and triggering lipid oxidation. Aqueous-phase species monitored in the phosphate solution included H_2O_2, O_3, NO_2^-, and NO_3^-. After dry air plasma treatment, NO_3^- was the dominant species in the phosphate solution, with a consistent amount across different pH levels. Increasing air humidity introduced H_2O_2 and elevated NO_2^- concentrations. However, the concentrations of H_2O_2, NO_2^-, and NO_3^- were not in line with the monitored lipid oxidation parameters.

It is then illustrated that lipid oxidation in emulsions is mainly induced by the dissolved gaseous reactive species with the dominant role of ozone. The solubility of gaseous species can be associated with the ionic strength in the emulsion, which is affected by the pH and concentration of phosphate buffer. Finally, the reduction in the concentration of gaseous O_3 with elevated RH remarkably diminished the extent of oxidation in emulsions. The literature-reported solubility of O_3 and its decomposition into radicals (e.g., ${}^{\bullet}OH$) can explain the observed lipid oxidation degrees across different pH levels (Egorova et al., 2015). This suggests that (dissolved) O_3 was the major reactive species inducing lipid oxidation in the emulsion using the multi-hollow surface DBD setup.

This study provides insights into the interactions among gaseous species, aqueous species, and lipid oxidation, as well as how these interactions are influenced by the intrinsic properties of the emulsion and the humidity of the plasma. O/W emulsions containing 10 wt% sunflower oil were used as the model system, while the effects of O/W ratio and oils with different degrees of unsaturation should be further investigated for specific food applications. Future studies should evaluate the effects of NTP in more complex food matrices, including mayonnaise, salad dressings, dairy emulsions, and beverage emulsions. Other food components, such as proteins, carbohydrates, and minerals, may interact with plasma-generated reactive species and consequently influence lipid oxidation, emulsion stability, and microbial inactivation. Understanding these matrix effects will facilitate the translation of findings from model systems to real food applications. Before commercial application, further toxicological assessments are needed including evaluation of N-nitrosamine formation from nitrite and in vitro study of cytotoxicity, mitochondrial dysfunction, and intestinal inflammatory responses.

CRediT authorship contribution statement

Danyang Liu: Writing – original draft, Methodology, Investigation, Formal analysis, Data curation, Conceptualization. **Oswaldo F. Lescano-Osorio:** Writing – review & editing, Methodology, Formal analysis, Data curation. **Anton Nikiforov:** Writing – review & editing, Supervision, Methodology, Investigation. **Nathalie De Geyter:** Writing – review & editing, Supervision, Resources, Project administration, Methodology, Funding acquisition, Conceptualization. **Zdenko Machala:** Writing – review & editing, Supervision, Methodology, Investigation. **Bruno De Meulenaer:** Writing – review & editing, Supervision, Resources, Project administration, Methodology, Funding acquisition, Conceptualization.

Funding

This research was funded by The Special Research Fund of Ghent University, grant number 01G00120, and the Slovak Research and Development Agency grant APVV-22-0247.

Declaration of competing interest

The authors declare that they have no known competing financial interests or personal relationships that could have appeared to influence the work reported in this paper.

Acknowledgement

This work was supported by COST Action CA19110 “PlAgri” (European Cooperation in Science and Technology). The authors would like to thank the Particle and Interfacial Technology Group (PaInT) of the Department of Green Chemistry and Technology at Ghent University for providing access to the Mastersizer 3000.

Appendix A. Supplementary data

Supplementary data to this article can be found online at https://doi.org/10.1016/j.ifset.2026.104828.

Data availability

Data will be made available on request.

References

Baird, R. B., Eaton, A. D., & Rice, E. W. (2017). *Standard methods for the examination of water and wastewater, 23rd Edition*. American Public Health Association. https://doi.org/10.1016/s0095-9561(16)33485-5

Bao, Y., & Pignitter, M. (2023). Mechanisms of lipid oxidation in water-in-oil emulsions and oxidomics-guided discovery of targeted protective approaches. *Comprehensive Reviews in Food Science and Food Safety, 22*(4), 2678–2705. https://doi.org/10.1111/1541-4337.13158

Bayati, M., Lund, M. N., Tiwari, B. K., & Poojary, M. M. (2024). Chemical and physical changes induced by cold plasma treatment of foods: A critical review. *Comprehensive Reviews in Food Science and Food Safety, 23*(4), Article e13376. https://doi.org/10.1111/1541-4337.13376

Bruggeman, P., & Schram, D. C. (2010). On OH production in water containing atmospheric pressure plasmas. *Plasma Sources Science and Technology, 19*(4), Article 045025. https://doi.org/10.1088/0963-0252/19/4/045025

Cimerman, R., & Hensel, K. (2023). Multi-hollow surface dielectric barrier discharge: Production of gaseous species under various air flow rates and relative humidity. *Plasma Chemistry and Plasma Processing, 43*(6), 1411–1433. https://doi.org/10.1007/s11090-023-10381-4

Dharini, M., Jaspin, S., Jagan, R., & Mahendran, R. (2022). Characterization of volatile aroma compounds in cold treated milk. *Journal of Food Processing and Preservation, 46*, Article e17059. https://doi.org/10.1111/jfpp.17059

Dharini, M., Jaspin, S., & Mahendran, R. (2023). Cold plasma reactive species: Generation, properties, and interaction with food biomolecules. *Food Chemistry, 405* (Part A), Article 134746. https://doi.org/10.1016/j.foodchem.2022.134746

Egorova, G. V., Voblikova, V. A., Sabitova, L. V., Tkachenko, I. S., Tkachenko, S. N., & Lunin, V. V. (2015). Ozone solubility in water. *Moscow University Chemistry Bulletin, 70*(5), 207–210. https://doi.org/10.3103/S0027131415050053

Frankel, E. N. (2005). *Lipid oxidation* (2nd ed.). The Oily Press.

Fridman, A. (2008). *Plasma chemistry*. Cambridge University Press.

Goldstein, S., Lind, J., & Merényi, G. (2005). Chemistry of peroxynitrites as compared to peroxynitrates. *Chemical Reviews, 105*(6), 2457–2470. https://doi.org/10.1021/cr0307087

Hennebelle, M., Villeneuve, P., Durand, E., Lecomte, J., van Duynhoven, J., Meynier, A., Yesiltas, B., Jacobsen, C., & Berton-Carabin, C. (2024). Lipid oxidation in emulsions: New insights from the past two decades. *Progress in Lipid Research, 94*, Article 101275. https://doi.org/10.1016/j.plipres.2024.101275

Ikawa, S., Tani, A., Nakashima, Y., & Kitano, K. (2016). Physicochemical properties of bactericidal plasma-treated water. *Journal of Physics D: Applied Physics, 49*, Article 425401. https://doi.org/10.1088/0022-3727/49/42/425401

Jadhav, H. B., Annapure, U. S., & Deshmukh, R. R. (2021). Non-thermal technologies for food processing. *Frontiers in Nutrition, 8*, Article 657090. https://doi.org/10.3389/fnut.2021.657090

Janda, M., Hensel, K., Peter, T., Hassan, M. E., & Machala, Z. (2021). The role of HNO2 in the generation of plasma-activated water by air transient spark discharge. *Applied Sciences, 11*, Article 7053. https://doi.org/10.3390/app11157053

Khuntia, S., Majumder, S. K., & Ghosh, P. (2015). Chemical engineering research and design quantitative prediction of generation of hydroxyl radicals from ozone microbubbles. *Chemical Engineering Research and Design, 98*, 231–239. https://doi.org/10.1016/j.cherd.2015.04.003

Kim, J. Y., Yi, B. R., Lee, C., Gim, S. Y., Kim, M. J., & Lee, J. H. (2016). Effects of pH on the rates of lipid oxidation in oil–water system. *Applied Biological Chemistry, 59*(2), 157–161. https://doi.org/10.1007/s13765-015-0146-3

ten Klooster, S., Boerkamp, V. J. P., Hennebelle, M., van Duynhoven, J. P. M., Schroën, K., & Berton-Carabin, C. C. (2024). Unravelling the effect of droplet size on lipid oxidation in O/W emulsions by using microfluidics. *Scientific Reports, 14*(1), 8895. https://doi.org/10.1038/s41598-024-59170-9

Korachi, M., Ozen, F., Aslan, N., Vannini, L., Guerzoni, M. E., Gottardi, D., & Ekinci, F. Y. (2015). Biochemical changes to milk following treatment by a novel, cold atmospheric plasma system. *International Dairy Journal, 42*, 64–69. https://doi.org/10.1016/j.idairyj.2014.10.006

Li, R., Dai, T., Zhou, W., Fu, G., Wan, Y., McClements, D. J., & Li, J. (2020). Impact of pH, ferrous ions, and tannic acid on lipid oxidation in plant-based emulsions containing saponin-coated flaxseed oil droplets. *Food Research International, 136*, Article No.109618. https://doi.org/10.1016/j.foodres.2020.109618

Liu, D., Sierens, J., Haydamous, C., Nikiforov, A., De Geyter, N., & De Meulenaer, B. (2024). Impact of nonthermal plasma treatment on the oxidation of lipids with different unsaturation degrees. *Journal of Agricultural and Food Chemistry, 72*(36), 20037–20047. https://doi.org/10.1021/acs.jafc.4c04365

Liu, D., Van Paepeghem, C., Sierens, J., Narimisa, M., Nikiforov, A., De Geyter, N., … De Meulenaer, B. (2023). Impact of nonthermal plasma on lipid oxidation from the perspective of plasma treatment parameters and plasma species: Identification of key reactive species. *Journal of Agricultural and Food Chemistry, 71*(38), 14057–14067. https://doi.org/10.1021/acs.jafc.3c03706

Liu, Z. C., Liu, D. X., Luo, S. T., Wang, W. T., Liu, Z. J., Yang, A. J., … Kong, M. G. (2019). The effect of pH on the aqueous reactive species in sodium phosphate buffers induced by surface air discharge. *Journal of Physics D: Applied Physics, 52*, Article 415201. https://doi.org/10.1088/1361-6463/ab2f07

Lukes, P., Dolezalova, E., Sisrova, I., & Clupek, M. (2014). Aqueous-phase chemistry and bactericidal effects from an air discharge plasma in contact with water: Evidence for the formation of peroxynitrite through a pseudo-second-order post-discharge reaction of H_2O_2 and HNO_2. *Plasma Sources Science and Technology, 23*(1), Article 015019. https://doi.org/10.1088/0963-0252/23/1/015019

Machala, Z., Tarabova, B., Hensel, K., Spetlikova, E., Sikurova, L., & Lukes, P. (2013). Formation of ROS and RNS in water electro-sprayed through transient spark discharge in air and their bactericidal effects. *Plasma Processes and Polymers, 10*(7), 649–659. https://doi.org/10.1002/ppap.201200113

Machala, Z., Tarabová, B., Sersenová, D., Janda, M., & Hensel, K. (2019). Chemical and antibacterial effects of plasma activated water: Correlation with gaseous and aqueous reactive oxygen and nitrogen species, plasma sources and air flow conditions. *Journal of Physics D: Applied Physics, 52*(3), Article 034002. https://doi.org/10.1088/1361-6463/aae807

Manchuri, K. M., Shaik, M. A., Subba, V., Gopireddy, R., Sultana, N., & Gogineni, S. (2024). Analytical methodologies to detect N - nitrosamine impurities in active pharmaceutical ingredients, drug products and other matrices. *Chemical Research in Toxicology, 37*, 1456–1483. https://doi.org/10.1021/acs.chemrestox.4c00234

McClements, D. J., & Decker, E. A. (2000). Lipid oxidation in oil-in-water emulsions: Impact of molecular environment on chemical reactions in heterogeneous food systems. *Journal of Food Safety, 65*(8), 1270–1282.

Misra, N. N., & Jo, C. (2017). Applications of cold plasma technology for microbiological safety in meat industry. *Trends in Food Science and Technology, 64*, 74–86. https://doi.org/10.1016/j.tifs.2017.04.005

Nikmaram, N., & Keener, K. M. (2022). The effects of cold plasma technology on physical, nutritional, and sensory properties of milk and milk products. *Journal of Food Science and Technology, 154*, Article 112729. https://doi.org/10.1016/j.lwt.2021.112729

Pareek, P., Kooshki, S., Tóth, P., & Janda, M. (2024). Tuning composition of plasma activated water generated by transient spark discharge with electrospray. *Chemical Engineering Journal, 493*, Article 152583. https://doi.org/10.1016/j.cej.2024.152583

Pawłat, J., Terebun, P., Kwiatkowski, M., Tarabová, B., Kovaľová, Z., Kučerová, K., … Janda, M. (2019). Evaluation of oxidative species in gaseous and liquid phase generated by mini - gliding arc discharge. *Plasma Chemistry and Plasma Processing, 39*(3), 627–642. https://doi.org/10.1007/s11090-019-09974-9

Sander, R. (2023). Compilation of Henry's law constants (version 5.0.0) for water as solvent. *Atmospheric Chemistry and Physics, 23*(19), 10901–12440. https://doi.org/10.5194/acp-23-10901-2023

Schmidt-bleker, A., Bansemer, R., & Reuter, S. (2016). How to produce an NOx- instead of ox- based chemistry with a cold atmospheric plasma jet. *Plasma Processes and Polymers, 13*(11), 1120–1127. https://doi.org/10.1002/ppap.201600062

Sierens, J., Narimisa, M., Demeestere, K., Heugebaert, T., Nikiforov, A., Geyter, N., & Meulenaer, B. (2026). Unraveling the reactive oxygen and nitrogen species responsible for oxidation of methionine, cysteine, tyrosine and tryptophan in atmospheric pressure nonthermal plasma treatment. *Journal of Agricultural and Food Chemistry, 74*(4), 3917–3935. https://doi.org/10.1021/acs.jafc.5c12473

Tarabová, B., Lukeš, P., Janda, M., Hensel, K., Šikurová, L., & Machala, Z. (2018). Specificity of detection methods of nitrites and ozone in aqueous solutions activated by air plasma. *Plasma Processes and Polymers, 15*(6), Article 1800030. https://doi.org/10.1002/ppap.201800030

Vandemoortele, A., & De Meulenaer, B. (2015). Behavior of malondialdehyde in oil-in-water emulsions. *Journal of Agricultural and Food Chemistry, 63*, 5694–5701. https://doi.org/10.1021/acs.jafc.5b01780

Verlackt, C. C. W., Van Boxem, W., & Bogaerts, A. (2018). Transport and accumulation of plasma generated species in aqueous solution. *Physical Chemistry Chemical Physics, 20*(10), 6845–6859. https://doi.org/10.1039/c7cp07593f

Villeneuve, P., Bourlieu-lacanal, C., Durand, E., Lecomte, J., Mcclements, D. J., Decker, E. A., … Lecomte, J. (2021). Lipid oxidation in emulsions and bulk oils: A review of the importance of micelles. *Critical Reviews in Food Science and Nutrition, 63*(20), 4687–4727. https://doi.org/10.1080/10408398.2021.2006138

Wandell, R. J., Wang, H., Bulusu, R. K. M., Gallan, R. O., & Locke, B. R. (2019). Formation of nitrogen oxides by nanosecond pulsed plasma discharges in gas-liquid reactors. *Plasma Chemistry and Plasma Processing, 39*, 643–666. https://doi.org/10.1007/s11090-019-09981-w

Wang, D., Xiao, H., Lyu, X., Chen, H., & Wei, F. (2023). Lipid oxidation in food science and nutritional health: A comprehensive review. *Oil Crop Science, 8*(1), 35–44. https://doi.org/10.1016/j.ocsci.2023.02.002

Wang, S., Zhang, J., Li, G., Ding, Y., Zhao, L., Song, Y., Duan, X., & Ge, W. (2022). Changes of bacterial microbiota and volatile flavor compounds in ewe milk during dielectric barrier discharge cold plasma processing. *Food Research International, 159*, Article 111607. https://doi.org/10.1016/j.foodres.2022.111607

WHO. (2016). *Nitrate and Nitrite in Drinking-water Background document for development of WHO Guidelines for Drinking-water Quality*.

Wu, X., Luo, Y., Zhao, F., Murad, M., .S., & Mu, G. (2021). Influence of dielectric barrier discharge cold plasma on physicochemical property of milk for sterilization. *Plasma Processes and Polymers, 18*(1), Article 1900219. https://doi.org/10.1002/ppap.201900219

Xiang, Q., Liu, X., Li, J., Liu, S., & Zhang, H. (2018). Effects of dielectric barrier discharge plasma on the inactivation of *Zygosaccharomyces rouxii* and quality of apple juice. *Food Chemistry, 254*(136), 201–207. https://doi.org/10.1016/j.foodchem.2018.02.008

Xing, W., Yin, M., Lv, Q., Hu, Y., Liu, C., & Zhang, J. (2014). Oxygen solubility, diffusion coefficient, and solution viscosity. In *Rotating Electrode Methods and Oxygen Reduction Electrocatalysts*. Elsevier B.V.. https://doi.org/10.1016/B978-0-444-63278-4.00001-X

Zhou, R., Zhou, R., Wang, P., Xian, Y., Mai-Prochnow, A., Lu, X., … Bazaka, K. (2020). Plasma activated water (PAW): Generation, origin of reactive species and biological applications. *Journal of Physics D: Applied Physics, 53*, Article 303001. https://doi.org/10.1088/1361-6463/ab81cf